IEEE Access
Multidisciplinary | Rapid Review | Open Access Journal

Received February 24, 2017, accepted March 27, 2017, date of publication April 18, 2017, date of current version June 7, 2017.

Digital Object Identifier 10.1109/ACCESS.2017.2695367

Vias and Stubs Loaded Patch and Its Applications in Filter and Rectifier Designs

BING JIE XIANG[1,2], WEN JU LIU[1,2], SHAO YONG ZHENG[1,2], (Member, IEEE), YONG MEI PAN[3], (Member, IEEE), YUAN XIN LI[1,2], (Member, IEEE), AND YUN LIANG LONG[1,2], (Senior Member, IEEE)

[1]School of Electronics and Information Technology, Sun Yat-sen University, Guangzhou 510006, China
[2]SYSU-CMU Shunde International Joint Research Institute, Shunde 528300, China
[3]School of Electronic and Information Engineering, South China University of Technology, Guangzhou 510640, China

Corresponding author: Shao Yong Zheng (e-mail: zhengshaoy@mail.sysu.edu.cn)

This work was supported in part by the National Natural Science Foundation of China under Grant 61671485, in part by the Science and Technology Program of Guangzhou, China, under Grant 201510010084, in part by the Fundamental Research Funds for the Central Universities under Grant 16lgzd04, and in part by the Guangdong Natural Science Foundation under Grant 2015A030312010.

ABSTRACT It is always advantageous to include additional bandpass filtering functionality within different circuits and components in the wireless communication system, and thus, a novel circular patch loaded with vias and stubs is proposed as the basic element to achieve this function integration, as well as the performance enhancement. Owing to the introduction of a new operation mode and flexibility of the proposed patch element in locating the frequencies of different operation modes, excellent bandpass characteristics can be implemented with simplicity in structure. First, the proposed patch element is used to implement a triple-mode bandpass filter with a very wide harmonic suppression. As an extension, a novel rectifying circuit with extended input power range and bandpass filtering property is implemented based on a bandpass filtering power divider, which is also implemented using the basic patch configuration. To verify the validity of the proposed patch configurations, three different kinds of circuits have been designed, fabricated, and measured. All measured results are found to be in good agreement with the simulation results.

INDEX TERMS Bandpass filter, rectifier, harmonic suppression, function integration.

I. INTRODUCTION

The idea of the microstrip patch was first introduced as an antenna by Deschamps in 1953. However, patch antennas did not attract much attention by researchers until the early 1970's. The succedent advances have made it one of the most widely used antennas in the wireless communication systems [1], [2]. This is because it provides many advantages compared to other conventional antennas, such as ease of construction, strong mechanical structure, low profile, and low cost, and so on.

Inspired by all these advantages, the patch element was considered for the implementation of microwave circuits. As the simplest case, the patch element is firstly utilized as the resonator in a bandpass filter. Different shapes of microstrip patch resonators have been proposed, such as square, circular and triangular patch elements [3]–[5]. Besides, patch elements have also been employed for the implementation of a quadrature coupler. Similarly, rectangular, circular, elliptical and circular sector shaped patch elements were reported respectively [6]–[9]. The previous patch based circuits usually suffer from a narrow operational bandwidth and large circuit size. Thus several approaches had been proposed to address these two issues. For the narrow bandwidth issue, stubs are loaded on rectangular patch coupler to provide the dual band operation [10]. While the patterned ground plane structure was introduced to compress the circuit size without increasing circuit complexity [11]. As an extension, the varactor diodes were loaded on the patterned ground plane to implement frequency agility [12] and function reconfigurability [13] for narrow bandwidth and large size issues respectively. However, the operating mode of the patch element used in these circuits is either TM_{11} or TM_{21} mode. As a result, the flexibility of these patch based circuits is limited.

In this paper, a new patch element is proposed as the fundamental component to realize different types of circuits with excellent performance and high integration level. Shorting vias are loaded on a circular patch element to introduce additional TM_{01} mode, which has not been reported in the

previous patch based circuits. Open stubs are loaded on the patch element to improve the selectivity of the bandpass and also introduce another operating mode. Based on this basic element, a triple-mode filter with both excellent bandpass filtering and very wideband harmonic suppression characteristics can be implemented. To further demonstrate the flexibility of proposed patch element, a power divider with additional excellent filtering function and high-order harmonic suppression is implemented and applied in a rectifying circuit. The input power range of the rectifying circuit is widened together with an excellent bandpass characteristic owing to the introduction of the proposed power divider.

This paper is organized as follow. The working principle of a vias and stubs loaded patch element is explained in Section II. And a triple-mode bandpass filter with a wide stopband up to 10th harmonic is proposed in Section III. As an extension, a power divider with bandpass filtering characteristic is implemented and applied in a rectifier for power range extension and function integration, as described in Section IV. Finally, a conclusion has been drawn in Section V.

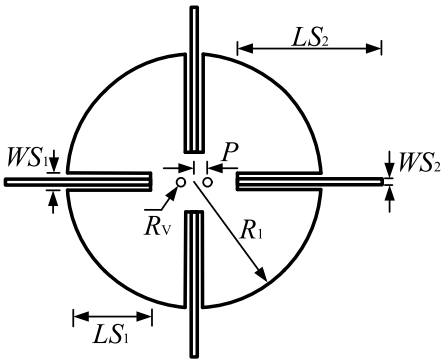

FIGURE 1. The configuration of the basic patch element.

II. THE VIAS AND STUBS LOADED PATCH ELEMENT

Fig. 1 shows the configuration of the basic patch element, which is a slotted circular patch with two shorting vias and four open stubs loaded. The four slots with the width of WS_1 and the length of LS_1 are loaded on the circular patch with a radius of R_1 across the horizontal and vertical planes. Two vias with a radius of R_V are located symmetrically on the patch, which is indicated by P. Four open stubs with the same width of WS_2 and the length of LS_2 are inserted into the slots. Owing to the simplicity and symmetry in structure, this basic patch element can be analyzed theoretically and further utilized to implement different types of circuits easily.

To investigate the working principle of the proposed vias and stubs loaded patch element, the behavior of a single mode resonator based on a circular patch is evaluated. As an example, a circular patch with a radius of 20 mm is implemented using Rogers RO4003C substrate with dielectric constant ε_r of 3.38 and thickness h of 0.813 mm. The 50 Ω input/output ports are connected to the patch resonator

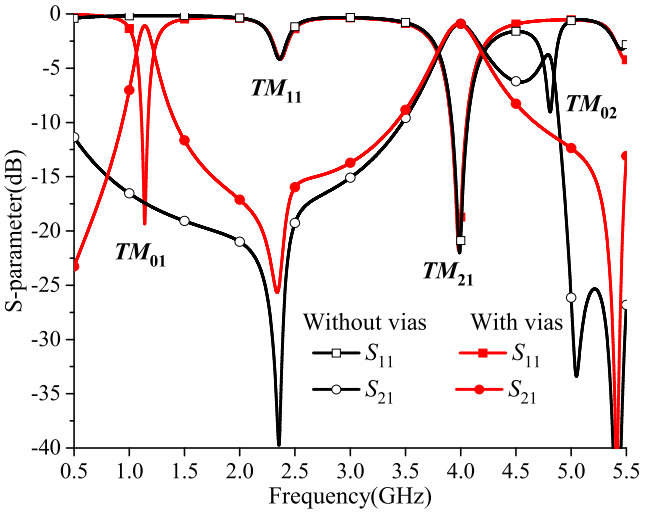

FIGURE 2. Frequency responses of the filters based on a circular patch with and without vias.

directly. The shorting vias with a radius of 0.5 mm are located at the position P, which is 0.7 mm away from the center. The frequency responses of the resonator with and without vias are shown in Fig. 2. Several resonant modes can be observed within the operating frequency band when the shorting vias are loaded on the patch element. They can be determined as TM_{01}, TM_{11}, TM_{21} and TM_{02} respectively according to the theory given in [14]–[16]. Fig. 3 shows the current distribution within the patch under different resonant modes. It can be observed that the introduction of vias does not affect the existing TM_{11} and TM_{21} modes, but introduces a new resonant mode located at 1.1 GHz, which has not been reported in the previous patch based circuits. For example, only TM_{11} and TM_{21} modes are utilized in the snowflake shaped patch [15] to implement a quadrature coupler. As the current direction on the patch will rotate with the different radii for the circular sector patch elements, the TM_{11} mode can be used to implement a bandpass filter [17], [18]. The three operating modes of the proposed bandpass filter in [17] and [18] are TM_{11}^x, TM_{11}^y and TM_{21}. Different from this, a transmission zero and pole coincide in resonant mode TM_{11} in this proposed configuration. This is because the direction of current flow is vertical to the port 2, which means very little energy will be transferred to port 2, as shown in Fig. 3. (b). Therefore, the TM_{01} and TM_{21} modes are considered here alternatively.

The introduction of the TM_{01} mode can improve the suppression within the lower stopband. When the vias are not loaded on the circular patch, the resonant frequency for the lowest mode (TM_{01}) of the patch element is zero [14]. The transmission coefficient (S_{21}) of the filter will climb up gradually with the decreasing frequency starting from the resonant frequency of TM_{11} mode, as depicted in Fig. 2. This results in the poor out of band suppression for the lower band. Similar phenomena can be found in the two designs reported in [15] and [17]. As shown in Fig. 2, the frequency

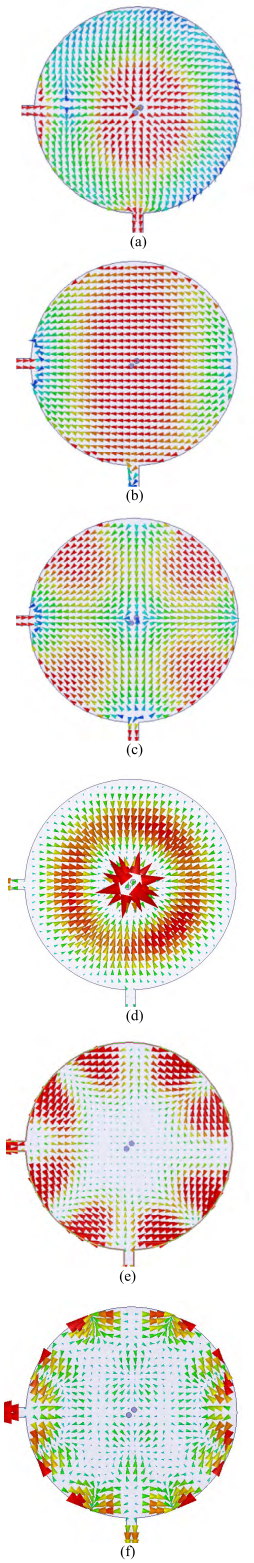

FIGURE 3. Current distributions within the circular patch. (a) TM_{01} mode (b) TM_{11} mode (c) TM_{21} mode (d) TM_{02} mode (e) TM_{41} mode (f) TM_{81} mode.

for the TM_{01} mode is shifted from zero to 1.1 GHz with the introduction of vias. Since there is no resonant mode within

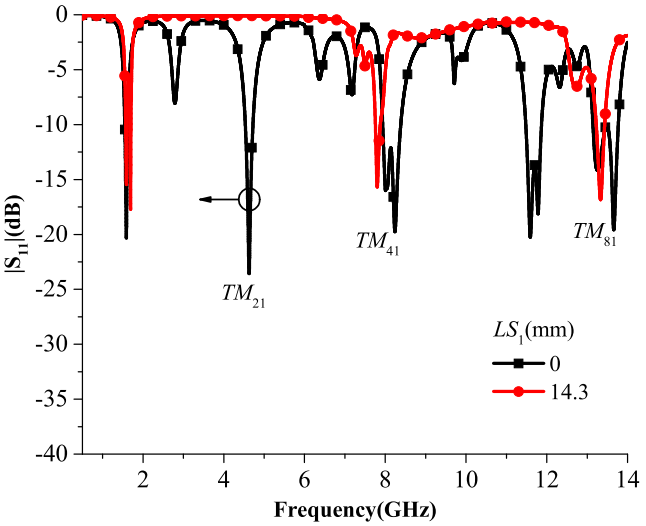

FIGURE 4. Simulated frequency responses of the basic patch filter with different LS_1.

the lower band, it can be concluded that the out of band suppression is improved by the loaded vias. The resonant frequencies of the vias loaded circular patch are determined by the following equation [14], [16]:

$$f_{mn} = \frac{k_{mn} \cdot c}{2\pi R \cdot \sqrt{\varepsilon_r}} \tag{1}$$

where the indexes m and n represent the corresponding TM mode, c is the velocity in the free space, ε_r is the relative permittivity of the substrate and k_{mn} are the roots of the following characteristic equation:

$$J_m'(k_{mn})N_m(k_{mn}g) - J_m(k_{mn}g)N_m'(k_{mn}) = 0 \tag{2}$$

where g is the ratio P/R_1 and $J_m(x)$ and $N_m(x)$ are the first and second kind mth order Bessel functions and the prime denotes the first derivative.

The TM_{21} mode should be properly controlled to approach the TM_{01} mode for the implementation of the multi-mode operation and wide stop band. As the current under TM_{01} mode flows in the radial direction, the slots do not affect the current path of TM_{01} mode, the resonant frequency of TM_{01} remains unchanged with slots loaded. While the slot can effectively lengthen the current path under the TM_{21} mode [15], resulting in a decrease in frequency of the TM_{21} mode. This property can be demonstrated by the simulated results shown in Fig. 4, in which TM_{11} and TM_{21} have been merged with each other. Therefore the implementation of a dual mode bandpass filter with good out of band suppression becomes possible. To introduce additional resonant mode within the passband and a transmission zero within the suppression band, four open quarter-wavelength stubs are loaded on the previous dual mode patch resonator [19], [20]. Because the two modes (TM_{01} and TM_{21}) are not affected by the loaded stubs, the implementation of triple-mode bandpass characteristics becomes possible. It should be emphasized that the working principle for the

proposed patch element is different from those reported in [17] and [18], a better selectivity can be achieved by introducing the TM_{01} mode and open stubs.

Besides the control of operating frequency for the TM_{21} mode, the slots can suppress some higher order modes of the circular patch simultaneously for the implementation of wideband harmonic suppression. Fig. 4 shows the frequency responses of the basic patch filter with different LS_1. With the four slots loaded, the current paths on the patch for different modes will be affected. The high-order modes except the TM_{41} and TM_{81} modes are suppressed by the disturbing of current paths. This is because only the current paths under TM_{41} and TM_{81} modes are almost in parallel with the slots, as shown in Figs. 3. (e) and 3. (f). According to Fig. 4, when the slots with a proper length are loaded, the high-order can be suppressed except the TM_{41} (7.8 GHz) and TM_{81} (13.3 GHz) modes. In this way, by properly controlling the dimensions of the slots and stubs, a triple-mode bandpass filter with a wide stopband can be implemented.

The operation principle of proposed patch element had been explained, the detailed analytical method should be provided as well. Since the proposed patch element is not a regular shape patch, the Green's function is not available in the literature. The planar component will be analyzed through the segmentation and desegmentation methods [21], [22]. Firstly, the proposed patch can be considered to be the combination of a slots and vias loaded circular patch α and four open stubs β as shown in Fig. 5. (a). However, the impedance matrix of the slot loaded patch α is still difficult to obtain. The sub-circuit α can be treated as a regular via loaded circular patch ζ with four rectangular patch γ subtracted, as indicated in Fig. 5. (b). The impedance matrix for α, β, γ and ζ segments are Z_α, Z_β, Z_γ, and Z_ζ respectively. According to the methods described in [21] and [22], the impedance matrix Z of the proposed vias and stubs loaded patch can be expressed by Z_β, Z_γ, and Z_ζ. As segment β, γ and ζ are all regular shapes, the corresponding impedance matrices $Z_{\beta,}Z_\gamma$, and Z_ζ can be obtained respectively [16].

Therefore, the impedance matrix of this basic vias and slots loaded patch can be calculated accordingly. Once the overall Z-matrix of this network is obtained, S-parameters characterization can be realized by using standard Z-matrix to S- matrix transformation.

III. TRIPLE-MODE PATCH BANDPASS FILTER WITH A WIDE HARMONIC SUPPRESSION BAND

A. COMPACT TRIPLE-MODE PATCH BANDPASS FILTER CONFIGURATION

With the emerging broadband communication systems, the demand for the wide bandwidth of bandpass filters has been unprecedentedly increasing. To accomplish the wideband characteristic, the most straightforward way is to cascade several patch resonators. But this will result in major drawbacks in terms of bulky size and high insertion loss. Alternatively, a multiple-mode resonator is considered to achieve a compact size and wide bandwidth simultaneously [23], [24].

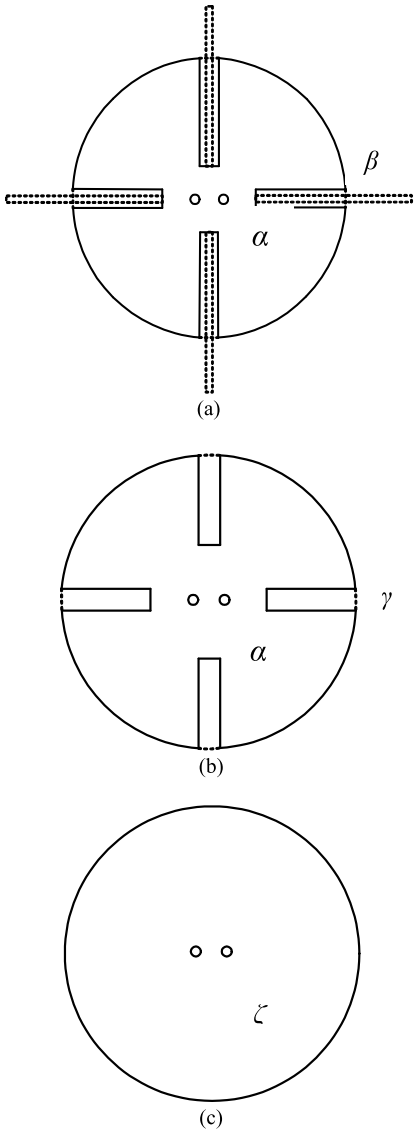

FIGURE 5. An illustration of the segmentation and desegmentation methods for the analysis of proposed patch element. (a) The first step of the segmentation and desegmentation methods. (b) The second step of the segmentation and desegmentation methods. (c) The third step of the segmentation and desegmentation methods.

To maintain a compact size, the microstrip line resonator with stubs loaded was proposed to realize the triple-mode filters [25]. For the implementation of a triple-mode bandpass filter on a patch element, four varactor diodes were loaded alternatively [17].

Besides the bandwidth issue, the harmonic suppression characteristic is also important for a bandpass filter, as the poor harmonic suppression may degrade the system performance. To suppress the harmonics of resonators, various methods have been proposed [26]–[32]. Substrate suspension [26] and wiggly lines [27] had been utilized to compensate the phase velocities for harmonic suppression. Another method is to use the individual stepped-impedance resonators (SIRs) with the same fundamental resonance frequency f_0 but different harmonic resonance frequencies [28]. The discriminating coupling

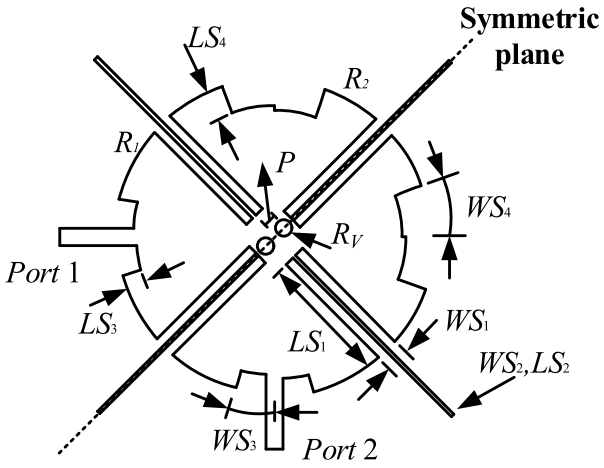

FIGURE 6. The configuration of the triple-mode bandpass patch filter with wide suppression band.

technique was proposed to suppress the second harmonic [29]. The spur lines were utilized for the harmonic suppression of stub loaded resonators alternatively [30]. A circular patch with four orthogonally oriented slots was proposed in [31], which extended the stopband to 4.66 f_0. However, the proposed circular patch filter only exhibits dual mode bandpass filtering property with a low harmonic suppression level. All these structures suffer from the narrow bandwidth or high design complexity caused by a large number of design parameters required. Therefore, a new structure is desired to implement the bandpass filter with a wide bandwidth, wide harmonic suppression band, and good frequency selectivity.

The operation principle of a vias and stubs loaded patch element had been explained in the previous section, the implementation of a bandpass filter can be obtained subsequently. Different feeding methods could be considered for this patch element. The most common feeding method, especially for planar structures, is the simple microstrip feed line. However, the input impedance at the input/output ports of the patch element is found to be lower than 50 Ω, an impedance transformer can be used but at the expense of a larger circuit size. Moreover, the suppression of the high-order harmonics should be taken into consideration in the feeding mechanism.

The configuration of the proposed patch bandpass filter is described in Fig. 6. Two feeding lines are inserted into the patch element orthogonally. Two slots are employed on the input/output ports as impedance transformers for simultaneous impedance matching and harmonic suppression. To investigate the effects of slots, the frequency responses of a bandpass filter with different slot length LS_3 are shown in Fig. 7. It can be found that the three operating modes are not affected by the slots, but the impedance matching deteriorates significantly when LS_3 varies to a smaller value. Figs. 7. (b) and 7. (c) show the frequency responses of the designed filter within the upper suppression band. It can be found that the introduction of slots can improve the suppression level of upper stopband significantly. When

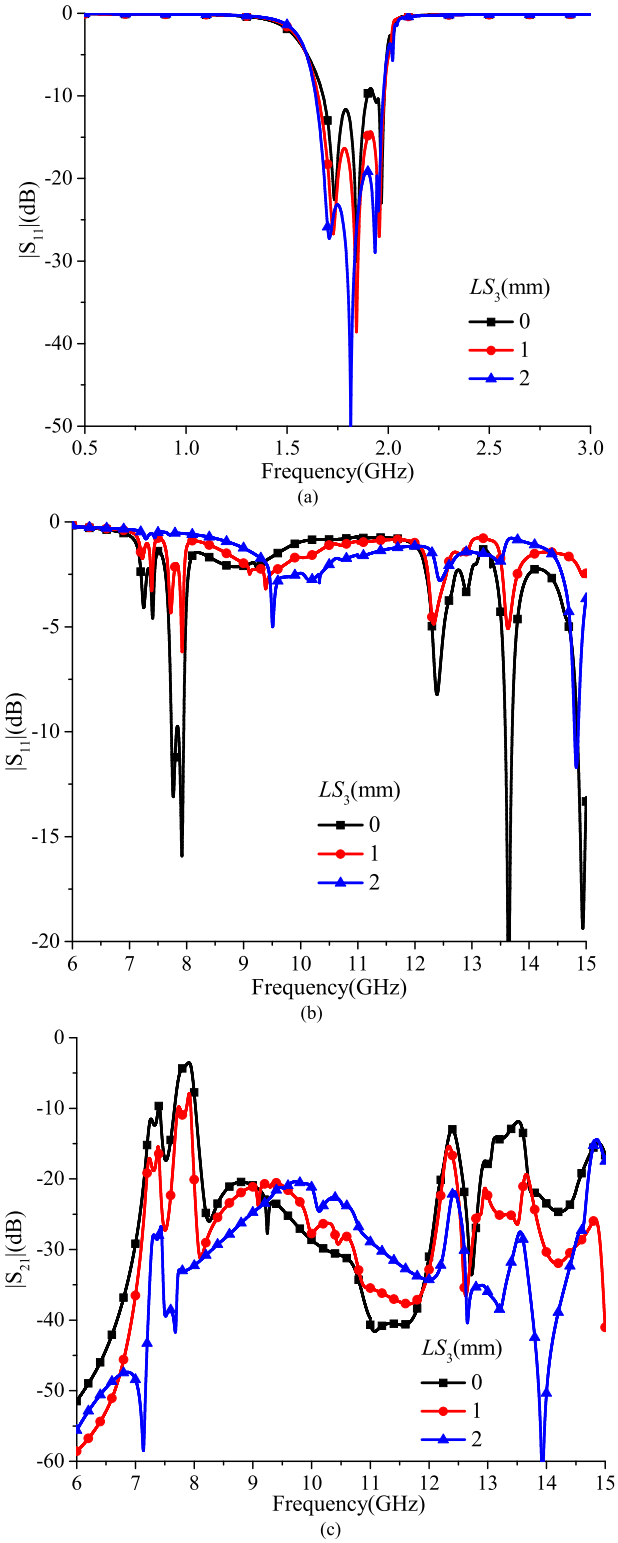

FIGURE 7. Simulated frequency responses of proposed triple-mode bandpass patch filter with different LS_3. (a) Simulated return losses around the pass band. (b) Simulated return losses within the stop band. (c) Simulated insertion losses within the stop band.

LS_3 increases from 0 mm to 2 mm, the stopband with a suppression level larger than 20 dB can be extended from 7 GHz (3.9f_0) to 14.5 GHz (8f_0). It can be concluded that

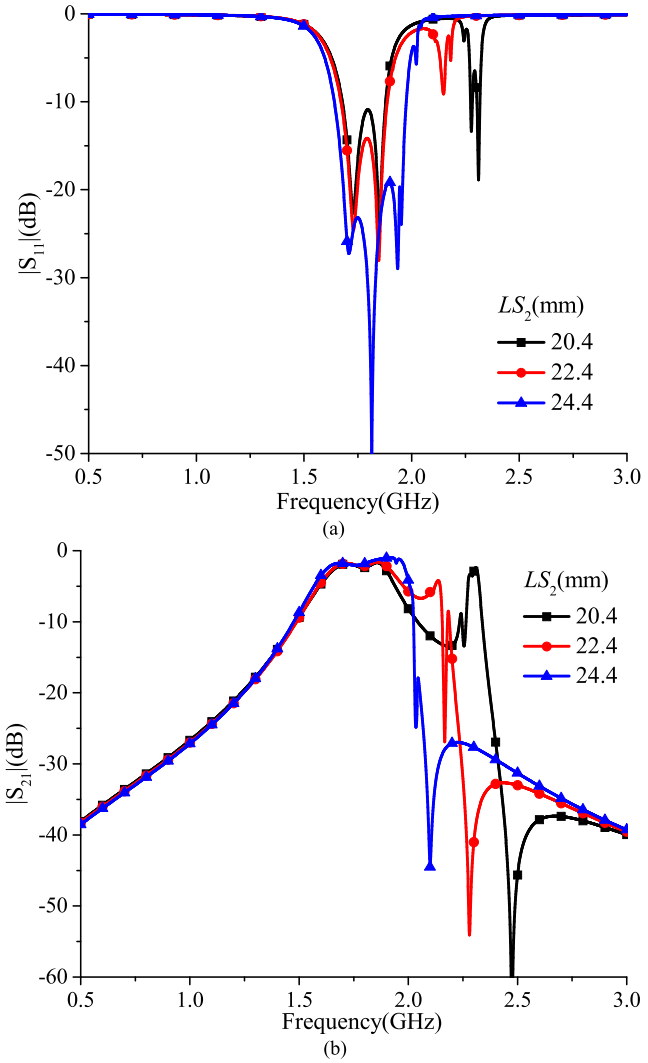

FIGURE 8. Simulated frequency responses of proposed triple-mode bandpass patch filter with different L_{s2}. (a) Simulated return losses. (b) Simulated insertion losses.

the slots are introduced on the input/output ports to obtain a better impedance matching within the passband and a high suppression level within the stopband simultaneously.

To verify the operating principle of the loading stubs given in the previous section, the parametric study on the parameters (LS_2) is also conducted in Fig. 8. It can be seen that the transmission zero moves from 2.5 GHz to 2.1 GHz with LS_2 increasing from 20.4 mm to 24.4 mm. At the same time, the frequency for the third mode moves from 2.3 GHz to 1.94 GHz. Therefore, the open stubs are responsible for enhancing the selectivity and introducing additional mode [19], [20].

B. DESIGN EXAMPLE AND EXPERIMENTAL RESULTS

For demonstration purposes, the design and experimental results of a triple-mode patch bandpass filter centered at 1.8 GHz, will be presented in this section. The circuit was fabricated using Rogers RO4003C with a dielectric constant of 3.38 and thickness of 0.813 mm. The dimensional circuit

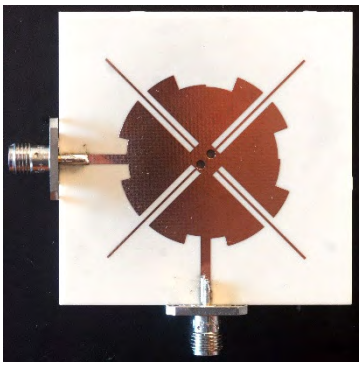

FIGURE 9. Photograph of the designed triple-mode patch bandpass filter.

parameters are $W_0 = 1.88$ mm, $R_1 = 17.4$ mm, $R_2 = 17$ mm, $R_V = 0.9$ mm, $WS_1 = 2.5$ mm, $LS_1 = 14.3$ mm, $WS_2 = 0.4$ mm, $LS_2 = 24.4$ mm, $WS_3 = 3.3$ mm, $LS_3 = 2$ mm, $WS_4 = 5.7$ mm, $LS_4 = 3.1$ mm, $P = 1.4$ mm. Fig. 9 shows the photograph of designed triple-mode patch bandpass filter. It is worth mentioning that the little difference between R_1 and R_2 are set for a better impedance matching, rather than exciting the degenerate mode of the circular patch.

The simulated and measured frequency responses of the triple-mode patch bandpass filter described above are shown in Fig. 10. Good agreement between simulated and experimental results is observed, which validates the proposed design. The circuit exhibits good return loss better than 10 dB within the passband from 1.64 GHz to 1.97 GHz. The insertion loss is smaller than 2 dB over the same band. The measured results show that the high suppression level ($|S_{21}| < -20$dB) can be found within the desired stopband up to 10^{th} harmonic frequency (18 GHz), which is much better than that of reconfigurable patch filter [17]. Within the lower stopband, the suppression level is high as 40 dB at 0.5 GHz, which is also much better than that of the reconfigurable patch filter [17]. Two transmission zeros with more than 30 dB suppression level are observed at about 2.03 GHz and 5.5 GHz, which are generated by the loading stubs and slots at input/output ports. The transmission zero at 2.03 GHz improves the selectivity of designed filter significantly.

Table 1 summarizes the comparison between the proposed patch filter and other related structures that can be found in the literature. First of all, the proposed structure achieves the widest stopband and largest suppression level compared to the previous patch based filters. Moreover, the bandwidth of the proposed filter (18.3%) is larger than those of the microstrip line based filters except [25]. Meanwhile, the stopband up to 10^{th} harmonic suppression is wider than those of the compared filters except [28]. Finally, the proposed patch filter exhibits a high simplicity in structure owe to the introduction of the new patch element, compared to other microstrip line based structures [25]–[30].

TABLE 1. Comparison between proposed patch filter and previous works.

Ref.	f_0 (GHz)	Technology	Insertion loss (dB)	No. of Modes	BW (%)	Harmonic suppression
[17]	2.4	Patch	2	3	31.5	> 15 dB up to 2.5th harmonic
[25]	1	Microstrip	1.62	3	27.2	> 20 dB up to 2th harmonic
[27]	2.5	Microstrip	-	2	10	> 20 dB up to 2.4th harmonic
[28]	1.5	Microstrip	2.52	2	8.9	> 23.7 dB up to 10.6th harmonic
[29]	2.4	Microstrip	2.4	2	12.5	> 30 dB up to 3.1th harmonic
[30]	2.4	Microstrip	0.78	3	15.8	> 20 dB up to 4th harmonic
[31]	0.8	Patch	0.778	2	33	> 10 dB up to 4.6th harmonic
This work	1.8	Patch	2	3	18.3	> 20 dB up to 10th harmonic

IV. BANDPASS FILTERING RECTIFIER WITH WIDE INPUT POWER RANGE

A. BANDPASS FILTERING RECTIFIER WITH WIDE INPUT POWER RANGE

Since the concept of wireless power transmission (WPT) has been proposed by Dr. Brown at the end of 1950's [32], the WPT technology has gained increasing interest since it is valuable for various potential applications [33]–[35]. The rectifier plays the most important role in the WPT system. Recently, different kinds of rectifying topologies have been intensively investigated around the world. For instance, class F load has been used as the output filter for efficiency enhancement [36], which is similar to the design concept of a Class-F amplifier. Besides, two-way rectifier structure also has been proposed for efficiency enhancement. A full-wave rectifying structure was employed to realize the high-efficiency rectifier [37]. A differentially driven rectifier structure has been proposed to gain higher efficiency [38]. However, most of these rectifiers can only maintain a high efficiency within a narrow input power range. In order to extend the operating power range of the rectifier, many solutions have been proposed. For example, a FET was introduced in the traditional rectifier as an adaptive switch to extend the operating power range [39], [40], but the operating frequency around 100 MHz may limit their practical applications. In [41], the power detector and switches are combined to achieve a high efficiency over a wide input power range. Besides the requirement in the input power range, the interference with the existing wireless communication systems should be avoided. Therefore, it is advantageous to integrate additional bandpass filtering functionality within the high efficiency rectifier.

To achieve all these characteristics, a two-way rectifier is proposed, as shown in Fig. 11. A bandpass power divider is employed to split the target input signal into two parts for rectifying, and reject the unwanted input signal to avoid the interference with existing wireless communications. To guarantee the high conversion efficiency, the class F loading approach is utilized. The combination of a $\lambda/4$ microstrip line and three open stubs is used as the dc pass filter. The lengths of open stubs are determined as quarter wave length at the fundament frequency, second and third harmonic frequencies respectively. The amplitudes of 4th and higher order harmonics are very low, and do not significantly contribute to the power loss, so the previous harmonic control is enough for a high conversion efficiency. Thus a power divider with bandpass filtering property is required for function integration and input power range extension. However, most of existing of power divider configurations do not exhibit additional bandpass filtering characteristics.

B. BANDPASS FILTERING POWER DIVIDER CONFIGURATION

The conventional approach to introduce additional bandpass filtering function is to insert bandpass filters between input/output ports and power divider, but this will result in a larger size and higher insertion loss. Recently, several designs have been proposed to achieve this integration. The main idea is to replace the transmission lines with different resonators, such as quarter-wavelength short-circuited resonators [42], net type resonators [43] and stub-loaded resonators [44].

Owe to the unique property of vias and stub loaded patch element, a bandpass filter with very wideband harmonic suppression has been implemented in the previous section. Thus the implementation of a bandpass power divider using the patch element is considered. The proposed configuration is shown in Fig. 12. Different from the filter configuration, the separation angle between ports are fixed to be 120° for

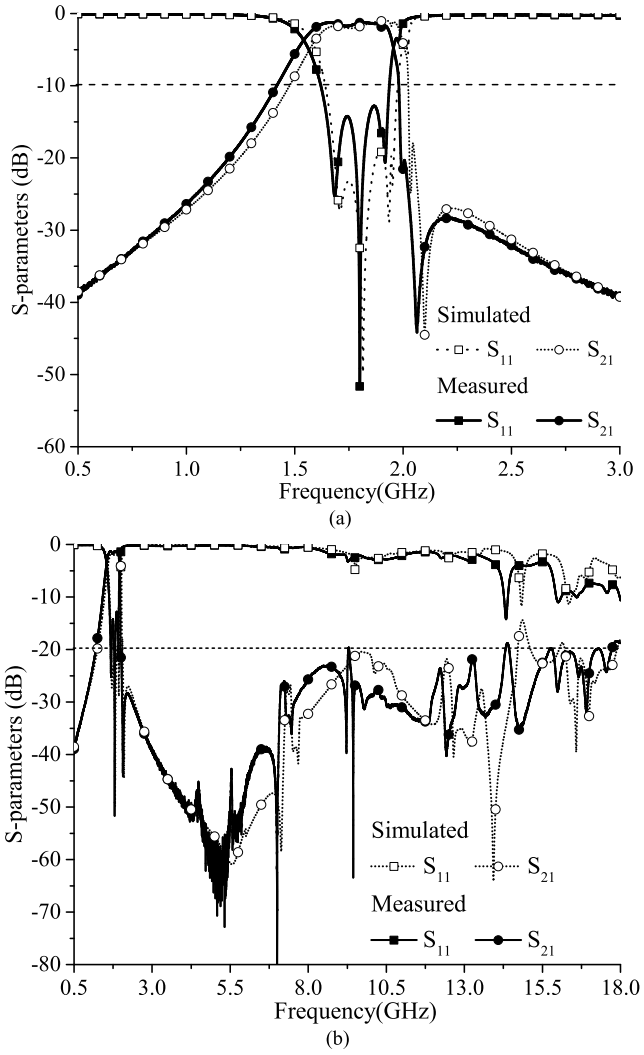

FIGURE 10. Simulated and measured responses of the designed triple-mode bandpass patch filter with wide suppression band. (a) narrow-band frequency response (b) wide-band frequency response.

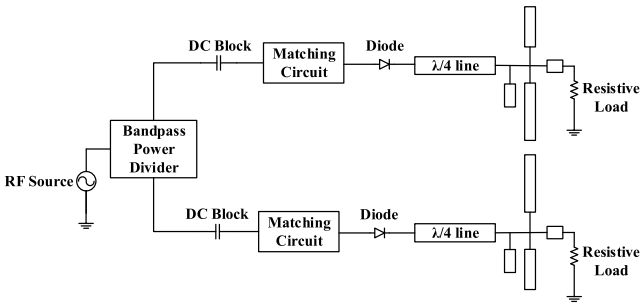

FIGURE 11. The schematic of the proposed bandpass filtering rectifier with a wide input power range.

symmetry, as indicated in the figure. The same vias and stub loaded circular patch is also utilized to implement a power divider with bandpass characteristics. For additional transmission zero and ease in impedance matching, the parameters for the slot and stub between port 2 and port 3 are arranged

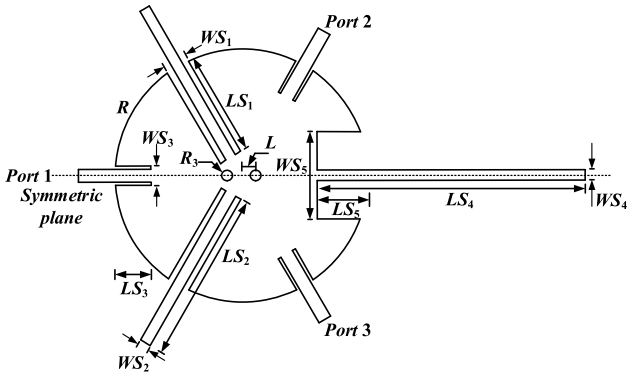

FIGURE 12. The configuration of the proposed bandpass power divider with wideband harmonic suppression.

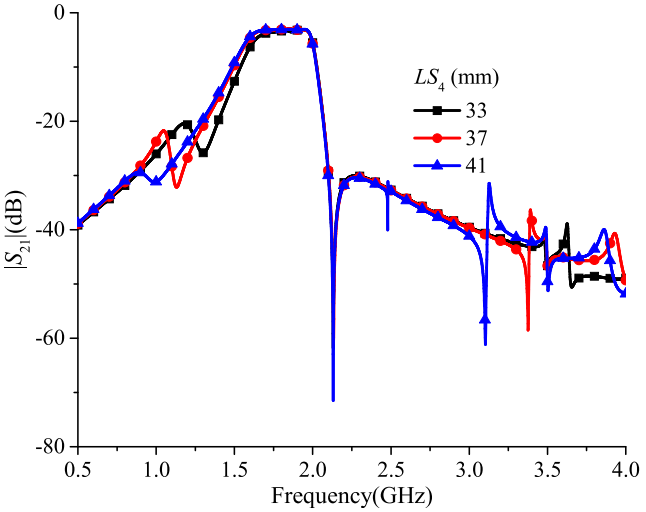

FIGURE 13. Simulated frequency responses of proposed bandpass patch power divider with different LS_4.

to be different from those for other slots and stubs between port 1 and port 2 or port 3. But the whole structure remains symmetric across the symmetric plane for equal power division. To get a further investigation on this proposed power divider, a parameter study is carried on.

Fig. 13 shows the simulated $|S_{21}|$ (dB) with varied stub length LS_4 with other parameters fixed. It can be observed that the transmission zero within lower suppression band can be controlled by the parameter LS_4. Since the working principle of this power divider is similar to that of the bandpass filter, which has been given in Section III, the power divider also shows a bandpass filtering characteristics and harmonic suppression. The three working modes are same as those of the bandpass filter, which are the TM_{01}, TM_{21} and another mode introduced by the quarter-wavelength open stub.

For demonstration purposes, a patch bandpass power divider is designed to operate at 1.8 GHz. The circuit was also fabricated using Rogers RO4003C substrate with a dielectric constant of 3.38 and thickness of 0.813 mm. The physical circuit parameters are: $W_0 = 1.88$ mm, $R = 17.5$ mm,

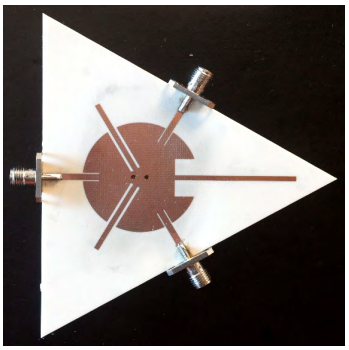

FIGURE 14. Photograph of the designed bandpass power divider.

$R_3 = 0.7$ mm, $WS_1 = 3.2$ mm, $LS_1 = 14.6$ mm, $WS_2 = 1.5$ mm, $LS_2 = 23.7$ mm, $WS_3 = 2.7$ mm, $LS_3 = 5$ mm, $WS_4 = 1.5$ mm, $LS_4 = 37$ mm, $WS_5 = 12$ mm, $LS_5 = 7$ mm, $L = 2$ mm. Fig. 14 shows the photograph of proposed circular based patch power divider with bandpass filtering characteristic.

Fig. 15 shows the simulated and measured frequency responses of the bandpass power divider described above. Good agreement between simulated and experimental results is observed, which validates our proposed design. The simulated and measured 10 dB impedance matching bandwidth are 18% (from 1.63-1.97 GHz) and 24.2% (1.56-1.99 GHz), respectively. The additional insertion loss is smaller than 1.5 dB over the whole passband. The measured results also show that the high suppression level ($|S_{21}| < -20$dB) can be found within the desired stopband up to 5th harmonic frequency (9.5 GHz). And two transmission zeros are observed at 1.2 GHz and 2.15 GHz within the lower and upper suppression bands respectively, which can improve the selectivity of the passband. Similar to the proposed filter, within the lower suppression band, the suppression level decreases to around 40 dB at 0.5 GHz due to the introduction of TM_{01} mode, which had been explained in Section II.

Table 2 summarizes the comparison between the proposed power divider with other structures that can be found in the literature. Compared to the microstrip line based power dividers [42]–[44], the patch based configuration can obtain a bandwidth of 24.2%, which is about 4 times of the bandwidth achieved by [42]. Meanwhile, the proposed patch power divider also exhibits a lower insertion loss compared to the previous works [43]. Small amplitude imbalance within the passband, high-frequency selectivity and a large rejection level within the suppression band are achieved in the proposed structure simultaneously. Moreover, the patch based configuration are more suitable for the high-frequency applications compared to the microstrip line based configuration owing to the ease of fabrication.

C. DESIGN EXAMPLE AND EXPERIMENTAL RESULTS

Based on the schematic of a bandpass rectifier and the new bandpass power divider configuration, a rectifier operating at 2.4 GHz is designed and fabricated using Rogers RO4003C

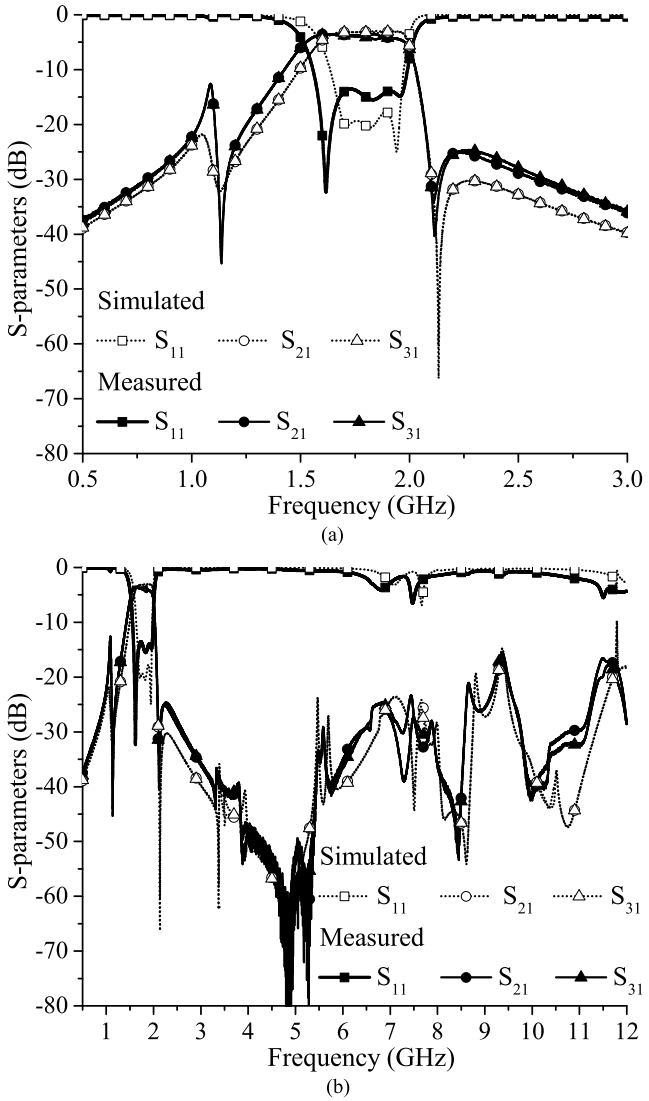

FIGURE 15. Simulated and measured responses of the designed bandpass patch power divider with wide suppression band. (a) narrow-band frequency response (b) wide-band frequency response.

substrate with a dielectric constant of 3.38 and thickness of 0.813 mm. A Schottky diode HSMS286b is chosen due to its low built-in voltage (0.3V) and high breakdown voltage (7V). Fig. 16 shows the configuration of the proposed rectifying circuit. The bandpass power divider proposed in the previous section is redesigned to operate at 2.4 GHz. The photograph of the fabricated rectifying circuit is shown in Fig. 17. The load resistance is determined as 1200 Ω. The bandpass rectifier circuit has been designed and optimized using the advanced design system (ADS) software, and the optimized parameters are (unit: millimeter): $W_0 = 1.38$, $R = 12.9$, $R_3 = 0.5$, $WS_1 = 2.4$, $LS_1 = 11.2$, $WS_2 = 1.7$, $LS_2 = 17.7$, $WS_3 = 2.2$, $LS_3 = 3.7$, $WS_4 = 1.1$, $LS_4 = 15.6$, $LS_6 = 10.5$, $WS_5 = 8.8$, $LS_5 = 5.1$, $L = 1.5$, $L_1 = 3$, $L_2 = 5.9$, $L_3 = 11.6$, $L_4 = 19$, $L_5 = 5.8$, $L_6 = 9$, $L_7 = 9$, $L_8 = 10.1$, $L_9 = 8.8$, $W_1 = 1.6$, $W_2 = 3.9$, $W_3 = 2.2$.

To demonstrate the effectiveness of proposed structure, a single way rectifier based on the same class F load approach

TABLE 2. Comparison between proposed power divider and previous works.

Reference	BW (%)	Insertion loss	No. of Transmission zeros	Harmonic Suppression
[42]	6.5	0.99	2	> 25 dB up to 2.4th harmonic
[43]	4.2	3	2	> 28 dB up to 5th harmonic
[44]	7.1	1.2	2	> 20 dB up to 2.9th harmonic
This Work	24.2	1.5	2	> 20 dB up to 5th harmonic

TABLE 3. Comparison between proposed rectifier and previous works.

Reference	Frequency	Diode	Input power range for eff >60% (mW)	Additional bandpass functionality	Harmonic Suppression
[36]	2.45 GHz	HSMS2860	1-20 mW	No	No
[38]	900 MHz	HSMS8202	5-30 mW	No	No
[39]	100 MHz	HSMS2860 /NE3210S01	0.1-126 mW	No	No
This Work	2.45 GHz	HSMS286b	7-45 mW	Yes	3rd

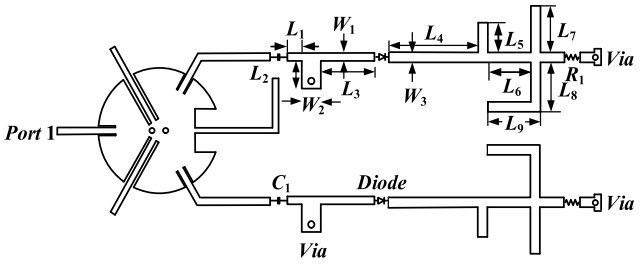

FIGURE 16. The topology of the proposed rectifying circuit.

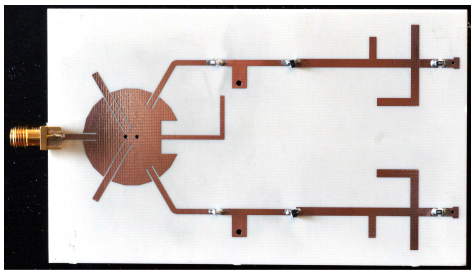

FIGURE 17. Photograph of the fabricated rectifying circuit.

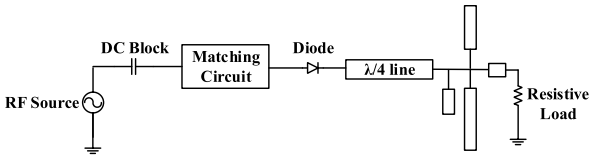

FIGURE 18. The schematic of a single way class F rectifier.

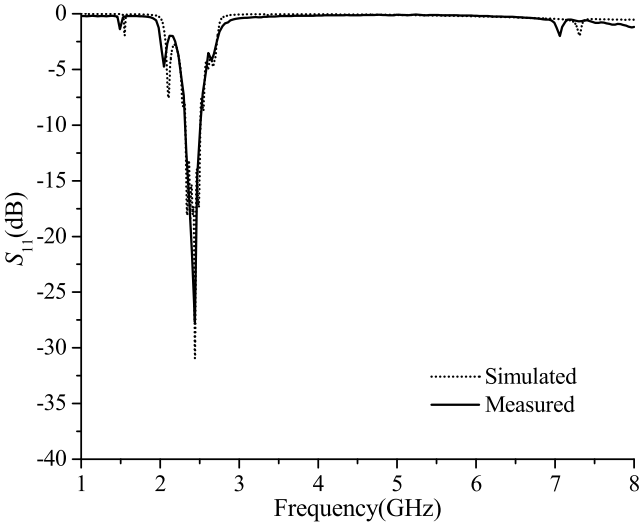

FIGURE 19. Simulated and measured return losses of the proposed rectifier.

is designed, fabricated and measured for further comparison. The schematic of this rectifier is shown in Fig. 18.

The simulated and measured input reflection coefficient and efficiency are depicted in Fig. 19. It can be observed that measured and simulated results agree with each other well. Measured efficiency and input reflection coefficient of the proposed rectifier are shown in Fig. 20. Only the signal at the specific frequency band will be converted to DC power, exhibiting good bandpass characteristics. In Fig. 21, the measured efficiency of the proposed rectifier and the single way rectifier are compared. The proposed rectifier topology

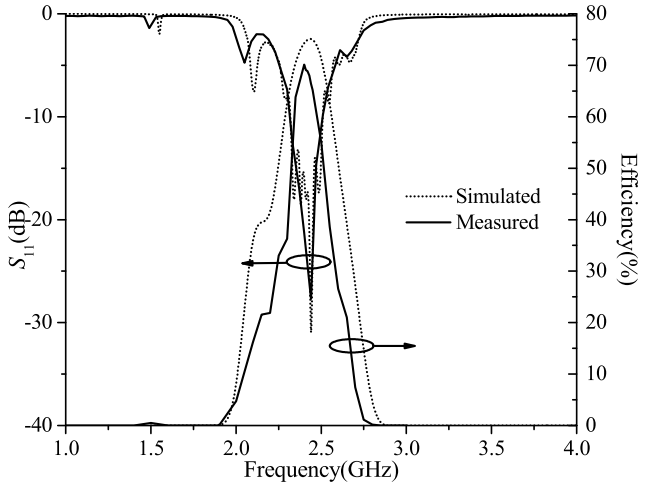

FIGURE 20. Simulated and measured efficiency and return losses of the proposed rectifier.

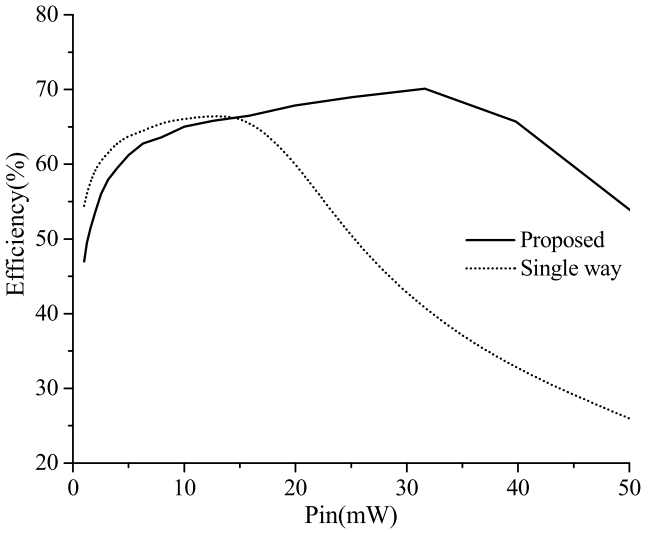

FIGURE 21. Measured efficiency of the proposed rectifier and the single way rectifier.

can significantly enhance the input power range maintaining an efficiency higher than 60%. The maximum conversion efficiency of the designed rectifier is 70.1% with the input power of 31.6 mW, which is larger than that of the single way one. These measured results show that the designed rectifier achieves a wide input power range and function integration simultaneously, which has not been reported previously.

In Table 3, the comparison between the proposed rectifier and several recently published works is conducted. Firstly, the proposed rectifier is the first configuration to realize input power range enhancement and bandpass filtering function integration simultaneously. The input power range for a conversion efficiency larger than 60% is 7 to 45 mW, which is wider than those of the rectifiers operating at microwave frequencies [36], [38]. The adaptive reconfigurable rectifier based on FET in [39] can achieve a wider input power range, but its operating frequency is low as 100 MHz, which may find limited applications. Moreover, the proposed structure achieves a wide stopband up to the 3rd harmonic.

V. CONCLUSION

In this paper, a basic structure based on a vias and stubs loaded circular patch with attractive behaviors have been presented and analyzed theoretically. The patch element has the advantages of high flexibility in the control of operation modes, which are particularly suitable for designing microwave circuits with bandpass filtering characteristics. By properly applying feed approach at the certain position of the patch, a triple-mode bandpass filter and bandpass power divider can then be designed. For demonstration, a triple-mode patch bandpass filter, and a power divider have been designed and fabricated. The measured results are all in good agreement with simulated predictions. Besides the desired characteristics within the passband, all designed circuits also exhibit a wide stopband. Furthermore, the designed power divider is applied to a rectifier for both input power range enhancement and bandpass function integration. This fundamental element can also be considered to implement other types of devices such as couplers, duplexers, antennas and so on. In addition, more feeding mechanisms such as coplanar waveguide fed and aperture coupled fed can be employed for performance enhancement.

REFERENCES

[1] K. F. Lee and K. M. Luk, *Microstrip Patch Antenna*. Singapore: World Sci., 2010.
[2] W. C. Mok, S. H. Wong, K. M. Luk, and K. F. Lee, "Single-layer single-patch dual-band and triple-band patch antennas," *IEEE Trans. Antennas Propag.*, vol. 61, no. 8, pp. 4341–4344, Aug. 2013.
[3] L. Zhu, P. M. Wecowski, and K. Wu, "New planar dual-mode filter using cross-slotted patch resonator for simultaneous size and loss reduction," *IEEE Trans. Microw. Theory Techn.*, vol. 47, no. 5, pp. 650–654, May 1999.
[4] B. T. Tan, S. T. Chew, M. S. Leong, and B. L. Ooi, "A modified microstrip circular patch resonator filter," *IEEE Microw. Wireless Compon. Lett.*, vol. 12, no. 7, pp. 252–254, Jul. 2002.
[5] J.-S. Hong and S. Li, "Theory and experiment of dual-mode microstrip triangular patch resonators and filters," *IEEE Trans. Microw. Theory Techn.*, vol. 52, no. 4, pp. 1237–1243, Apr. 2004.
[6] T. Kawai and I. Ohta, "Planar-circuit-type 3-dB quadrature hybrids," *IEEE Trans. Microw. Theory Techn.*, vol. 42, no. 12, pp. 2462–2467, Dec. 1994.
[7] M. E. Bialkowski and S. T. Jellett, "Analysis and design of a circular disc 3-dB coupler," *IEEE Trans. Microw. Theory Techn.*, vol. 42, no. 8, pp. 1437–1442, Aug. 1994.
[8] K.-L. Chan, F. A. Alhargan, and S. R. Judah, "A quadrature-hybrid design using a four-port elliptic patch," *IEEE Trans. Microw. Theory Techn.*, vol. 45, no. 2, pp. 307–310, Feb. 1997.
[9] S. Y. Zheng, J. H. Deng, Y. M. Pan, and W. S. Chan, "Circular sector patch hybrid coupler with arbitrary coupling coefficient and phase difference," *IEEE Trans. Microw. Theory Techn.*, vol. 61, no. 5, pp. 1781–1792, May 2013.
[10] Y. C. Li, H. Wong, and Q. Xue, "Dual-mode dual-band bandpass filter based on a stub-loaded patch resonator," *IEEE Microw. Wireless Compon. Lett.*, vol. 21, no. 10, pp. 525–527, Oct. 2011.
[11] S. Y. Zheng, S. H. Yeung, W. S. Chan, K. F. Man, and S. H. Leung, "Size-reduced rectangular patch hybrid coupler using patterned ground plane," *IEEE Trans. Microw. Theory Techn.*, vol. 57, no. 1, pp. 180–188, Jan. 2009.
[12] S. Y. Zheng, W. S. Chan, and K. F. Man, "Frequency agile patch element using varactor loaded patterned ground plane," *IEEE Trans. Microw. Theory Techn.*, vol. 59, no. 3, pp. 619–626, Mar. 2011.
[13] S. Y. Zheng, W. S. Chan, and Y. S. Wong, "Reconfigurable RF quadrature patch hybrid coupler," *IEEE Trans. Ind. Electron.*, vol. 60, no. 8, pp. 3349–3359, Aug. 2013.

[14] V. González-Posadas, D. Segovia-Vargas, E. Rajo-Iglesias, J. L. Vázquez-Roy, and C. Martín-Pascual, "Approximate analysis of short circuited ring patch antenna working at TM_{01} mode," *IEEE Trans. Antennas Propag.*, vol. 54, no. 6, pp. 1875–1879, Jun. 2006.

[15] S. Y. Zheng, Z. W. Liu, Y. M. Pan, Y. Wu, W. S. Chan, and Y. Liu, "Bandpass filtering doherty power amplifier with enhanced efficiency and wideband harmonic suppression," *IEEE Trans. Circuits Syst. I, Reg. Papers*, vol. 63, no. 3, pp. 337–346, Mar. 2016.

[16] R. Garg, P. Bhartia, I. Bahl, and A. Ittipiboon, *Microstrip Antenna Design Handbook*. Norwood, MA, USA: Artech House, 2001, p. 320, ch. 5.

[17] A. L. C. Serrano, F. S. Correra, T. P. Vuong, and P. Ferrari, "Analysis of a reconfigurable bandpass circular patch filter," *IEEE Trans. Microw. Theory Techn.*, vol. 58, no. 12, pp. 3918–3924, Dec. 2010.

[18] A. L. C. Serrano and F. S. Correra, "A triple-mode bandpass filter using a modified circular patch resonator," *Microw. Opt. Technol. Lett.*, vol. 51, no. 1, pp. 178–182, 2009.

[19] W.-H. Tu and K. Chang, "Compact second harmonic-suppressed bandstop and bandpass filters using open stubs," *IEEE Trans. Microw. Theory Techn.*, vol. 54, no. 6, pp. 2497–2502, Jun. 2006.

[20] S.-J. Sun, T. Su, K. Deng, B. Wu, and C.-H. Liang, "Compact microstrip dual-band bandpass filter using a novel stub-loaded quad-mode resonator," *IEEE Microw. Wireless Compon. Lett.*, vol. 23, no. 9, pp. 465–467, Sep. 2013.

[21] R. Chadha and K. C. Gupta, "Segmentation method using impedance matrices for analysis of planar microwave circuits," *IEEE Trans. Microw. Theory Techn.*, vol. 29, no. 1, pp. 71–74, Jan. 1981.

[22] P. C. Sharma and K. C. Gupta, "Desegmentation method for analysis of two-dimensional microwave circuits," *IEEE Trans. Microw. Theory Techn.*, vol. MTT-29, no. 10, pp. 1094–1098, Oct. 1981.

[23] W.-C. Tang and S. K. Chaudhuri, "A true elliptic-function filter using triple-mode degenerate cavities," *IEEE Trans. Microw. Theory Techn.*, vol. 32, no. 11, pp. 1449–1454, Nov. 1984.

[24] S. Bastioli and R. V. Snyder, "Inline pseudo elliptic $TE_{01\delta}$-mode dielectric resonator filters using multiple evanescent modes to selectively bypass orthogonal resonators," *IEEE Trans. Microw. Theory Techn.*, vol. 60, no. 12, pp. 3988–4001, Dec. 2012.

[25] K. Srisathit, A. Worapishet, and W. Surakampontorn, "Design of triple-mode ring resonator for wideband microstrip bandpass filters," *IEEE Trans. Microw. Theory Techn.*, vol. 58, no. 11, pp. 2867–2877, Nov. 2010.

[26] J.-T. Kuo, M. Jiang, and H.-J. Chang, "Design of parallel-coupled microstrip filters with suppression of spurious resonances using substrate suspension," *IEEE Trans. Microw. Theory Techn.*, vol. 52, no. 1, pp. 83–89, Jan. 2004.

[27] T. Lopetegi *et al.*, "New microstrip 'Wiggly-Line' filters with spurious passband suppression," *IEEE Trans. Microw. Theory Techn.*, vol. 49, no. 9, pp. 1593–1598, Sep. 2001.

[28] C. H. Kim and K. Chang, "Wide-stopband bandpass filters using asymmetric stepped-impedance resonators," *IEEE Microw. Wireless Compon. Lett.*, vol. 23, no. 2, pp. 69–71, Feb. 2013.

[29] X. Y. Zhang, X. Dai, H.-L. Kao, B.-H. Wei, Z. Y. Cai, and Q. Xue, "Compact LTCC bandpass filter with wide stopband using discriminating coupling," *IEEE Trans. Compon., Packag., Manuf. Technol.*, vol. 4, no. 4, pp. 656–663, Apr. 2014.

[30] A. Torabi and K. Forooraghi, "Miniature harmonic-suppressed microstrip bandpass filter using a triple-mode stub-loaded resonator and spur lines," *IEEE Microw. Wireless Compon. Lett.*, vol. 21, no. 5, pp. 255–257, May 2011.

[31] Y. K. Singh and A. Chakrabarty, "Miniaturized dual-mode circular patch bandpass filters with wide harmonic separation," *IEEE Microw. Wireless Compon. Lett.*, vol. 18, no. 9, pp. 584–586, Sep. 2008.

[32] W. C. Brown, "The history of power transmission by radio waves," *IEEE Trans. Microw. Theory Techn.*, vol. 32, no. 9, pp. 1230–1242, Sep. 1984.

[33] V. Kuhn, C. Lahuec, F. Seguin, and C. Person, "A multi-band stacked RF energy harvester with RF-to-DC efficiency up to 84%," *IEEE Trans. Microw. Theory Techn.*, vol. 63, no. 5, pp. 1768–1778, May 2015.

[34] C. H. P. Lorenz, S. Hemour, and K. Wu, "Physical mechanism and theoretical foundation of ambient RF power harvesting using zero-bias diodes," *IEEE Trans. Microw. Theory Techn.*, vol. 64, no. 7, pp. 2146–2158, Jul. 2016.

[35] Y. Huang, N. Shinohara, and T. Mitani, "A constant efficiency of rectifying circuit in an extremely wide load range," *IEEE Trans. Microw. Theory Techn.*, vol. 62, no. 4, pp. 986–993, Apr. 2014.

[36] J. Guo, H. Zhang, and X. Zhu, "Theoretical analysis of RF-DC conversion efficiency for class-F rectifiers," *IEEE Trans. Microw. Theory Techn.*, vol. 62, no. 4, pp. 977–985, Apr. 2014.

[37] U. Olgun, C.-C. Chen, and J. L. Volakis, "Investigation of rectenna array configurations for enhanced RF power harvesting," *IEEE Antennas Wireless Propag. Lett.*, vol. 10, pp. 262–265, Apr. 2011.

[38] H. Sun, "An enhanced rectenna using differentially-fed rectifier for wireless power transmission," *IEEE Antennas Wireless Propag. Lett.*, vol. 15, pp. 32–35, Feb. 2016.

[39] H. Sun, Z. Zhong, and Y.-X. Guo, "An adaptive reconfigurable rectifier for wireless power transmission," *IEEE Microw. Wireless Compon. Lett.*, vol. 23, no. 9, pp. 492–494, Sep. 2013.

[40] H. C. Sun, Z. Zhong, and Y. X. Guo, "Design of rectifier with extended operating input power range," *Electron. Lett.*, vol. 49, no. 18, pp. 1175–1176, Aug. 2013.

[41] V. Marian, C. Vo lIaire, J. Verdier, and B. Allard, "Potentials of an adaptive rectenna circuit," *IEEE Antennas Wireless Propag. Lett.*, vol. 10, pp. 1393–1396, Dec. 2011.

[42] X. Y. Zhang, K.-X. Wang, and B.-J. Hu, "Compact filtering power divider with enhanced second-harmonic suppression," *IEEE Microw. Wireless Compon. Lett.*, vol. 23, no. 9, pp. 483–485, Sep. 2013.

[43] C.-F. Chen, T.-Y. Huang, T.-M. Shen, and R.-B. Wu, "Design of miniaturized filtering power dividers for system-in-a-package," *IEEE Compon., Packag., Manuf. Technol.*, vol. 3, no. 10, pp. 1663–1672, Oct. 2013.

[44] K. Song, "Compact filtering power divider with high frequency selectivity and wide stopband using embedded dual-mode resonator," *Electron. Lett.*, vol. 51, no. 6, pp. 495–497, Mar. 2015.

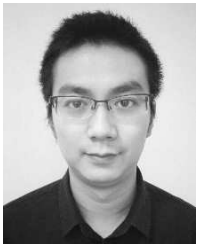

BING JIE XIANG was born in Chongqing, China. He received the B.S. degree in information engineering from the South China University of Technology, Guangzhou, China, in 2015. He is currently pursuing the M.Eng. degree with Sun Yat-sen University, Guangzhou. His current research interests include microwave circuits and antennas.

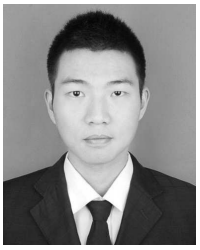

WEN JU LIU was born in Hubei, China. He received the B.S. degree in electronic science and technology from the Hebei University of Science and Technology, Hebei, China, in 2015. He is currently pursuing the M.Eng. degree with Sun Yat-sen University, Guangzhou, China. His current research interests include wireless power transfer and RF energy harvesting.

SHAO YONG ZHENG (S'07–M'11) was born in Fujian, China. He received the B.S. degree in electronic engineering from Xiamen University, Fujian, China, in 2003, and the M.Sc., M.Phil., and Ph.D. degrees in electronic engineering from the City University of Hong Kong, Kowloon, Hong Kong, in 2006, 2008, and 2011, respectively.

From 2011 to 2012, he was a Research Fellow with the Department of Electronic Engineering, City University of Hong Kong. He is currently an Associate Professor with the Department of Electronics and Communication Engineering, Sun Yat-sen University, Guangzhou, China. His research interests include microwave/millimeter wave circuits and evolutionary algorithms.

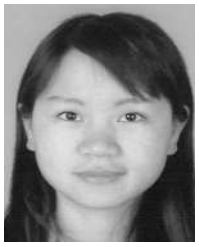

YONG MEI PAN (M'11) was born in Anhui, China, in 1982. She received the B.Sc. and Ph.D. degrees in electrical engineering from the University of Science and Technology of China, in 2004 and 2009, respectively.

From 2009 to 2012, she was a Research Fellow with the Department of Electronic Engineering, City University of Hong Kong. In 2013, she joined the School of Electronic and Information Engineering, South China University of Technology (SCUT) as an Associate Professor, where she is a currently a Professor. Her research interests include dielectric resonator antennas, leaky wave antennas, metasurface antennas, and filtering antennas.

YUAN XIN LI (M'08) was born in Guangzhou, China. He received the B.S. and Ph.D. degrees from Sun Yat-sen University, China, in 2001 and 2006, respectively.

From 2006 to 2008 and 2010, he was a Senior Research Assistant and Research Fellow with the State Key Laboratory of Millimeter Waves, City University of Hong Kong. In 2008, he joined the Department of Electronics and Communication Engineering, Sun Yat-sen University, where he is currently an Associate Professor. His research interests include microstrip leaky wave antenna and the applications of the periodic construction.

YUN LIANG LONG (M'01–SM'02) was born in Chongqing, China. He received the B.Sc., M.Eng., and Ph.D. degrees from the University of Electronic Science and Technology of China, Chengdu, in 1983, 1989, and 1992, respectively.

From 1992 to 1994, he was a Post-Doctoral Research Fellow, then employed as an Associate Professor, with the Department of Electronics, Sun Yat-sen University, Guangzhou, China. From 1998 to 1999, he was a Visiting Scholar with IHF, RWTH University of Aachen, Germany. From 2000 to 2001, he was a Research Fellow with the Department of Electronics Engineering, City University of Hong Kong, China. He is currently a Full Professor and the Head of the Department of Electronics and Communication Engineering, Sun Yat-sen University. He has authored and co-authored over 200 academic papers. His research interests include antennas and propagation theory, EM theory in inhomogeneous lossy medium, computational electromagnetics, and wireless communication applications.

Dr. Long is a member of the Committee of the Microwave Society of CIE, and on the Editorial Board of the *Chinese Journal of Radio Science*. He is a Vice Chairman of the Guangzhou Electronic Industrial Association.